




Resonant absorption in an inhomogeneous disordered metamaterial: First-principles simulationAlexander Zharov ^{*}*Université de Lorraine, CNRS, IJL, F-88000 Epinal, France**and Institute for Physics of Microstructures, Russian Academy of Sciences, Nizhny Novgorod 603950, Russia*Vanessa Fierro [‡] and Alain Celzard [†]*Université de Lorraine, CNRS, IJL, F-88000 Epinal, France*

(Received 17 January 2022; revised 21 April 2022; accepted 28 June 2022; published 11 July 2022)

In this study, we perform first-principles simulations of the resonant excitation of plasmalike oscillations in a two-dimensional inhomogeneous disordered metamaterial. The oscillations are initiated by an oblique incidence of a linearly polarized electromagnetic wave. The conditions for resonant excitation are satisfied near the point where the real part of the effective permittivity of the metamaterial changes sign from positive to negative and crosses zero. First, the problem was analyzed in the framework of the effective medium approximation, which predicts a resonant growth of the electric field and associated resonant absorption near the interface between positive and negative permittivity. It was shown that an array of point dipoles can sustain plasmalike waves near the zero of the effective permittivity. In order to trace the appearance of such a mode at the microscopic scale, full-scale first-principles simulations of a two-dimensional metamaterial with a randomly generated distribution and a linearly increasing average concentration of meta-atoms were performed. The results of the simulations were compared to the predictions of the effective medium approximation. The influence of the fluctuations in the meta-atom concentration on the excitation of the field oscillations and the resonant absorption was quantified.

DOI: [10.1103/PhysRevA.106.013504](https://doi.org/10.1103/PhysRevA.106.013504)**I. INTRODUCTION**

In modern electromagnetics, studies of metamaterials (MMs) occupy an important place as they pave the way for the control of electromagnetic fields at the micro- and nanoscales. Since the first studies [1,2] and until today, a variety of types of MMs have been proposed and fabricated, such as linear and nonlinear negative-index (or left-handed) MMs [3–8], tunable nonlinear and elastic MMs [9,10], plasmonic MMs [11–13], and artificial hyperbolic media [14–16]. Inspired by their very special properties, which are not found in natural materials, MMs have found a wide range of applications, including invisibility cloaking [17,18], superlensing [19,20], transformation optics [21,22], and enhancement of chirality and optical activity [23,24].

Historically, much attention has been paid to MMs with periodically ordered structural elements, called meta-atoms. Various methods have been formulated to quantify the propagation of electromagnetic waves in such systems [25–30]. Notably, a variety of homogenization techniques has been developed to simplify the macroscopic description of MMs [31–35]. At the same time, a large class of MMs, including liquid MMs [36–38], does not suggest periodicity, implying random variations in the parameters of meta-atoms or their spatial distribution. The properties of such disordered MMs have been extensively studied [39–41]. Different effective

medium approximations for random MMs have been elaborated [42–44]. Yet, the examination of the effects beyond the effective medium approximation is attractive from a theoretical point of view.

A particular case of interest is the analysis of electromagnetic systems that show a singular behavior within the effective medium approximations. An example of such a system can be an MM whose permittivity varies continuously. Indeed, near the zero-index transition point, i.e., the point where the effective refractive index crosses zero, anomalous field enhancement and resonant absorption have been predicted [45,46]. Similar effects are observed in inhomogeneous plasmas where the permittivity changes sign [47].

In this study, we perform first-principles simulations of a resonant excitation of plasmalike oscillations near the transition point in an inhomogeneous disordered two-dimensional (2D) MM. The MM is modeled as an array of randomly distributed meta-atoms, each of which is represented by a 2D ball (disc) with a Drude permittivity. The resonant mode is excited by an oblique incidence of a linearly polarized plane electromagnetic wave on a layer of MM with a linearly increasing average concentration of meta-atoms. As meta-atoms possess a negative polarizability in a certain frequency range above the plasmon resonance, the effective medium theory predicts the emergence of negative effective permittivity at sufficiently high meta-atom concentrations. As a result, with a linear increase in concentration, at a certain point the real part of the effective permittivity changes sign and crosses zero. This leads to the appearance of a resonant collective excitation near the transition point, along with the

^{*}alexander.zharov@univ-lorraine.fr[†]alain.celzard@univ-lorraine.fr

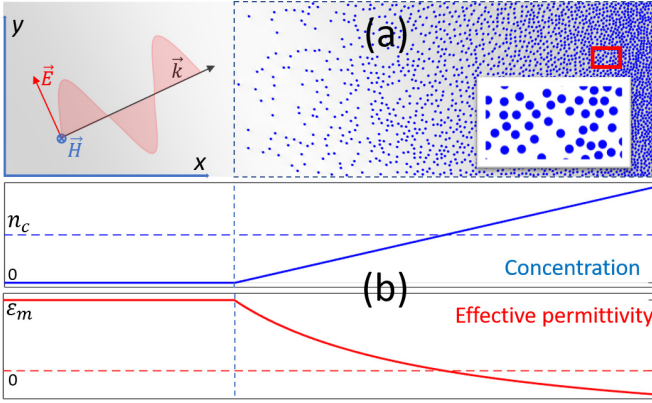


FIG. 1. (a) Schematic picture of the simulated system. An electromagnetic wave with E_x and E_y components of the electric field \mathbf{E} and H_z component of the magnetic field \mathbf{H} is incident on an MM with randomly distributed meta-atoms with linearly increasing concentration in the x direction. The dashed box shows the area occupied by the MM. When randomly seeded, the meta-atoms were prevented from overlapping and touching. The inset schematically shows the zoomed area enclosed by the red rectangle. (b) Qualitative plots of the meta-atom concentration (blue, upper subplot) and the effective permittivity (red, lower subplot). When the concentration reaches some critical value n_c , the real part of the effective permittivity crosses zero and becomes negative.

associated resonant absorption of the incident electromagnetic wave.

The paper is organized as follows: In Sec. II, we define the studied system and analyze it in the effective medium approximation in order to establish a reference for the following simulations. In Sec. III, we describe the simulations performed for several realizations of the randomly distributed meta-atoms, as well as for the effective medium, with the parameters obtained by homogenizing the randomly generated systems. In Sec. IV, we analyze the results of the simulations, compare them with the effective medium approximation, and discuss the effects beyond the homogenization theory. Finally, the conclusion section summarizes the results.

II. THEORETICAL EVALUATION

The studied system is an inhomogeneous MM with a random distribution of meta-atoms whose concentration is linearly dependent on a single coordinate. As this system will subsequently be a subject of full-scale numerical simulations, we consider a two-dimensional problem to remain within the limits of the available computational power. This has no qualitative effect and thus no loss of generality. The geometry of the problem is shown in Fig. 1(a). A linearly polarized electromagnetic wave with E_x and E_y components of the electric field \mathbf{E} and H_z component of the magnetic field \mathbf{H} is obliquely incident on a slab of inhomogeneous MM. The MM is composed of randomly distributed meta-atoms with an average concentration that increases linearly along the x axis. The meta-atoms are represented by circles and are therefore isotropic in two dimensions. We assume that the meta-atom

material has a Drude relative permittivity,

$$\epsilon_{MA}(\omega) = 1 - \frac{\omega_p^2}{\omega^2 + i\gamma\omega}, \quad (1)$$

where ω_p is the plasma frequency, ω is the frequency, γ is the damping factor, and i is the imaginary unit. Thus, the polarizability per unit length of such particles in the xy transverse plane can be written as follows:

$$\alpha_{MA}(\omega) = \frac{1}{4\pi} 2S_0 \frac{\epsilon_{MA}(\omega) - \epsilon_m}{\epsilon_{MA}(\omega) + \epsilon_m}, \quad (2)$$

where $S_0 = \pi r_0^2$ is the area of a meta-atom of radius r_0 and ϵ_m is the relative permittivity of the surrounding medium. At frequencies higher than the surface plasmon frequency, $\omega_{sp} = \omega_p / \sqrt{1 + \epsilon_m}$, the polarizability becomes negative [see Fig. 1(b)].

First, let us consider the problem within the continuous medium approximation. Assuming that the radii of the meta-atoms are much smaller than the wavelength, and that the number of meta-atoms on the wavelength scale is much larger than 1, i.e., $\lambda n^{1/2} \gg 1$, where n is the 2D concentration and λ is the wavelength, the meta-atom distribution can be treated as a continuous medium with an effective relative permittivity. As so far we are interested only in qualitative effects, we will use the simplest homogenization technique, namely, the Maxwell Garnett (MG) mixing formula, which in 2D takes the form

$$\epsilon_{\text{eff}}(\omega, x) = \epsilon_m \frac{1 + \overline{\rho(x)} \frac{\pi}{2} \frac{\epsilon_{MA}(\omega) - \epsilon_m}{\epsilon_{MA}(\omega) + \epsilon_m}}{1 - \overline{\rho(x)} \frac{\pi}{2} \frac{\epsilon_{MA}(\omega) - \epsilon_m}{\epsilon_{MA}(\omega) + \epsilon_m}}, \quad (3)$$

where $\overline{\rho(x)} = n(x)S_0$ is the average filling fraction of meta-atoms. Evidently, this formula does not account for the finite size of the meta-atoms or for any retardation effects. As follows from Eq. (3), in the frequency range where the polarizability is negative, the effective permittivity may also become negative at sufficiently high filling fractions. We will focus on this particular case, when, due to the increasing concentration of meta-atoms along the x axis, the effective permittivity becomes negative at some point.

The problem stated above has a strong resemblance to that of electromagnetic wave propagation in an inhomogeneous plasma, which was solved elsewhere [47]. It is indeed clear that the fields in these problems are governed by similar equations,

$$\frac{d^2 u}{dx^2} - \frac{1}{\epsilon_{\text{eff}}(x)} \frac{d\epsilon_{\text{eff}}(x)}{dx} \frac{du}{dx} + k_0^2 [\epsilon_{\text{eff}}(x) - q^2] u = 0, \quad (4)$$

where $k_0 = \omega/c$ is the wave number in vacuum, c is the speed of light, and $q = \sin \theta_0$, where θ_0 is the value of the incidence angle. The function u defines the magnetic and electric fields as follows:

$$H_z = u(x) e^{-i\omega t + ik_0 q y}, \quad (5)$$

$$E_x = \frac{1}{ik_0 \epsilon_{\text{eff}}(x)} \frac{\partial H_z}{\partial y}, \quad (6)$$

$$E_y = -\frac{1}{ik_0 \epsilon_{\text{eff}}(x)} \frac{\partial H_z}{\partial x}. \quad (7)$$

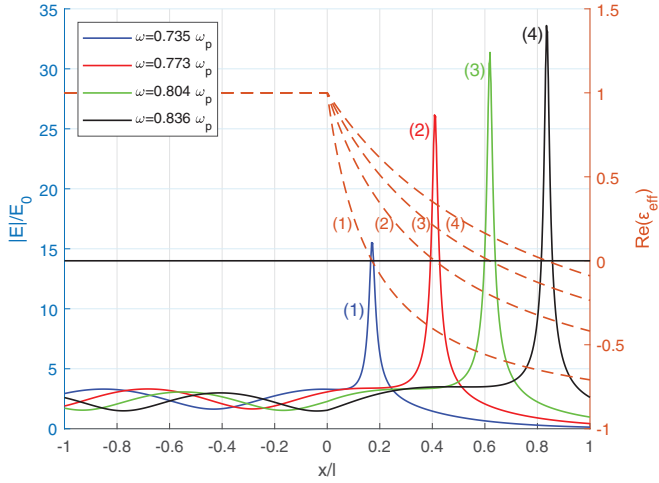


FIG. 2. Examples of distributions of the real part of dielectric permittivity (right scale, dashed lines) and the corresponding distribution of the normalized electric field (left scale, solid lines) for four different frequencies: $\omega = 0.735\omega_p$, $0.773\omega_p$, $0.804\omega_p$, and $0.836\omega_p$. The incidence angle was set to $\pi/7$.

It can be shown that $u(x)$ remains finite at the point x_0 where ϵ_{eff} crosses zero, which leads to the appearance of singularities in both E_x and E_y . Namely, E_x diverges as $1/(x - x_0)$, while E_y has a logarithmic divergence. Evidently, in a lossy material, the fields do not tend to infinity and grow to some maximum value, which is defined by the losses. It should be noted that the resonant growth of the electric field only takes place at the oblique incidence of the electromagnetic wave. Indeed, according to Eq. (6), the most divergent component of the electric field, E_x , is proportional to $q = \sin \theta_0$, which disappears at normal incidence, $\theta_0 = 0$. Moreover, as shown in [47] and references therein, the singular logarithmic term in E_y is also proportional to q , and also disappears at normal incidence. As a result, at normal incidence, the resonant increase of the field does not appear. At the same time, at sufficiently high values of the incidence angle θ_0 , the maximum of the electric field is suppressed because of the exponential decay of $u(x)$ between the reflection point defined by $\epsilon_{\text{eff}}(x) - q^2 = 0$ and the point of singularity, $\epsilon_{\text{eff}}(x) = 0$. Thus, for further calculations, we have arbitrarily set the value of the incident angle to $\pi/7$. Examples of the electric field distribution are shown in Fig. 2.

The associated total resonant absorption W can be calculated by integrating the electromagnetic power loss density, $1/2\text{Re}(\mathbf{j}\mathbf{E}^*)$, as follows:

$$W = \frac{1}{2} \int \text{Re}(\mathbf{j}\mathbf{E}^*) dx = \frac{1}{2} \int \text{Re}(\sigma) |\mathbf{E}|^2 dx, \quad (8)$$

where \mathbf{j} is the current density and σ is the effective electrical conductivity of the medium. The integration can be performed by substituting (6) and (7) into (8) and approximating the real part of the permittivity as a linear function crossing zero. As a result, the total absorption W can be estimated as follows:

$$W = \frac{\pi}{2k_0^2} \frac{\text{Re}(\sigma)}{\text{Re}(d\epsilon_{\text{eff}}/dx) \text{Im}(\epsilon_{\text{eff}})} \left| \frac{\partial H_z}{\partial y} (x = x_0) \right|^2. \quad (9)$$

Given that the real part of the conductivity can be expressed as $\text{Re}(\sigma) = \omega \text{Im}(\epsilon_{\text{eff}})$, we obtain that $\text{Im}(\epsilon_{\text{eff}})$ in Eq. (9) cancels out. Therefore, the resonant absorption does not depend on the imaginary part of the permittivity, which means that even though the losses may have a different origin or value, the total absorption remains the same as long as the other parameters are similar. Such a behavior is common for resonant systems, as changing the losses simultaneously changes the width and the height of the resonant peak while keeping the integral Eq. (8) unchanged.

Although the problem statements for plasma and MM are seemingly very similar, the microscopic mechanisms underlying the enhancement of the electric field are different. In plasma, charge separation is possible and is responsible for the increase of the macroscopic electric field near the surface where the real part of the permittivity crosses zero. Indeed, when the real part of the permittivity is zero, the electrostatic plasma oscillations can be resonantly excited, leading to the rapid growth of the electric field. The width of this resonance and the amplitude of the field oscillations are defined by the losses.

On the other hand, in a MM, charge separation is only possible within the meta-atoms, which are assumed to be small compared to any other scale of the problem. In other words, the MM considered here can be generally treated as an array of point dipoles, which do not allow for macroscopic charge separation. Therefore, the macroscopic increase in the electric field must be attributed to the excitation of a collective dipole mode, which may propagate in the MM. To understand this, consider a 2D MM with randomly distributed meta-atoms. Assuming that the excitation propagates along the x axis as a longitudinal wave, it will induce the polarization of meta-atoms in the x direction with the dipole moment, $\mathbf{p}(\mathbf{r}_m) = \hat{\mathbf{x}} p \exp(ikx_m)$, where $\mathbf{r}_m = (x_m, y_m)$ are the coordinates of the m th meta-atom, $\hat{\mathbf{x}}$ represents the unit vector along the x axis, p is the dipole moment value, and k is the wave vector.

A dipole positioned at an observation point $\mathbf{r} = (x, y)$ is subject to the electric field produced by all the other dipoles, which can be expressed by the following sum:

$$\mathbf{E}(\mathbf{r}) = \sum_m \frac{4\delta\mathbf{r}_m(\mathbf{p}(\mathbf{r}_m)\delta\mathbf{r}_m)}{\delta r_m^4} - \frac{2\mathbf{p}(\mathbf{r}_m)}{\delta r_m^2}, \quad (10)$$

where $\delta\mathbf{r}_m = \mathbf{r} - \mathbf{r}_m$ is the vector connecting the m th dipole and the observation point. Substituting the expression for the dipole moments, the electric field takes the form

$$\mathbf{E}(\mathbf{r}) = \hat{\mathbf{x}} E(\mathbf{r}) = \hat{\mathbf{x}} e^{ikx} \sum_m p e^{-ik\delta r_m \cos \phi_m} \frac{4 \cos^2 \phi_m - 2}{\delta r_m^2}, \quad (11)$$

where ϕ_m is the angle between $\mathbf{p}(\mathbf{r}_m)$ and $\delta\mathbf{r}_m$. As we are interested in the field averaged over the spatial variations of the dipole distribution, the summation can be approximated by integration, leading to

$$E(\mathbf{r}) = 2pn e^{ikx} \int_{\bar{l}}^{\infty} \delta r d\delta r \int_0^{2\pi} d\phi e^{-ik\delta r \cos \phi} \frac{2 \cos^2 \phi - 1}{\delta r^2}, \quad (12)$$

where n is again the concentration of meta-atoms, i.e., the number of meta-atoms per unit area, and $\bar{l} = n^{-1/2}$ is the

average distance between the meta-atoms, which plays the role of cutoff distance. The integration thus gives

$$E(\mathbf{r}) = -4\pi p n e^{ikx} \frac{J_1(k\bar{l})}{k\bar{l}}, \quad (13)$$

where $J_1(z)$ is the first-order Bessel function.

Finally, the self-consistency restriction requires that $p(\mathbf{r}) = \alpha_{MA}(\omega)E(\mathbf{r})$, which provides us with the condition for the existence of a special eigenmode, a self-correlated longitudinal dipole wave analogous to a plasma wave:

$$1 + \rho \frac{\varepsilon_{MA}(\omega) - \varepsilon_m}{\varepsilon_{MA}(\omega) + \varepsilon_m} \frac{J_1(k\bar{l})}{\pi k\bar{l}} = 0. \quad (14)$$

It can be seen that the propagation of such waves is governed solely by spatial dispersion, while otherwise they reduce to simultaneous dipole oscillations in the entire space. Nevertheless, in the nondispersive limit $k\bar{l} \rightarrow 0$, Eq. (14) reduces to $1 + \rho \frac{\pi}{2} \frac{\varepsilon_{MA}(\omega) - \varepsilon_m}{\varepsilon_{MA}(\omega) + \varepsilon_m} = 0$, which reads exactly as $\varepsilon_{\text{eff}} = 0$. Thus, the increase in the electric field near the transition point is attributed to the resonant excitation of plasmlike longitudinal waves sustained by the dipole oscillations.

III. SIMULATION

The simulations were performed using COMSOL MULTIPHYSICS (Electromagnetic Waves, Frequency Domain solver). The system was modeled by randomly seeding 2485 circular meta-atoms with linearly increasing concentration on a rectangle with an aspect ratio of 2.43. When randomly seeded, the particles were prevented from overlapping and touching. The permittivity of the meta-atoms was simulated by the Drude model. The angle of incidence was set to $\pi/7$.

Figure 3 shows the electric field distribution at different frequencies. It can be seen that at each frequency, there is an area of maximum average field, which corresponds to the satisfaction of condition (14).

The dependence of the field distribution on the real-time frequency change is available in the Supplemental Material [48].

Figure 4 shows the frequency dependence of the transmission and reflection coefficients averaged over five random realizations and the absorption as a function of the damping factor at different frequencies. The irregular behavior of the reflection and transmission in Fig. 4(a) is evidently a consequence of the random character of the considered system. The absorption, given by Fig. 4(b), depends weakly on the damping factor of the meta-atom material and varies between 0.6 and 0.8 depending on the frequency.

It is interesting to trace the similarities between the excited modes in the homogenized and random systems with similar average parameters. The comparison between the simulations of the MG approximation and the random system at different frequencies is shown in Fig. 5.

Figure 6 shows the comparison of the averaged electric field distributions for MG approximation and random distribution. The averaging was performed over the entire y coordinate and with the Gaussian smoothing function over the x coordinate.

Finally, to verify that the simulation results do not qualitatively depend on a particular realization of the meta-atom

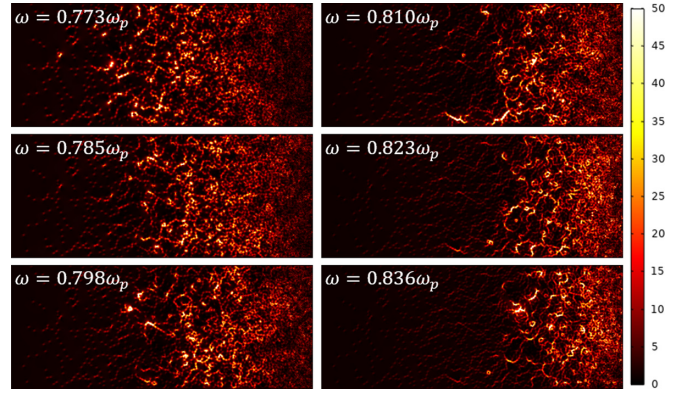


FIG. 3. Electric field distribution in the MM system shown in Fig. 1 illuminated by an electromagnetic wave at different frequencies. The wave polarization and orientation of axes are the same as in Fig. 1. The frequencies were set to $\omega = 0.773\omega_p$, $0.785\omega_p$, $0.798\omega_p$, $0.810\omega_p$, $0.823\omega_p$, and $0.836\omega_p$, as indicated in the upper left corner of each subimage. The incidence angle was set to $\pi/7$. The number of meta-atoms is 2485. The meta-atom distribution was randomly generated with a concentration increasing linearly in the x direction; the meta-atoms were prevented from overlapping and touching. The color bar represents the absolute value of the electric field normalized by the incident wave amplitude. It should be noted that the color scale is limited to 50 for ease of reading the figure, while the actual maximum of the normalized electric field reaches approximately 250.

distribution, several random distributions generated by the same randomization procedure were simulated. The comparison of these simulations is shown in Fig. 7.

The averaged field distributions in the random systems shown in Fig. 7 are presented in Fig. 8.

IV. DISCUSSION

The problem considered here is of interest as it sheds light on how collective modes appear in random MMs without turning to effective medium approximations.

First, as can be seen in Fig. 3, with the increase of the electromagnetic wave frequency, the resonant region moves to the areas of higher meta-atom concentration. This observation

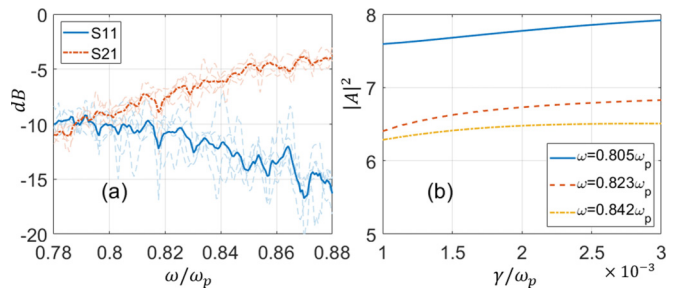


FIG. 4. (a) Reflection (blue solid line) and transmission (red dot-dashed line) coefficients of the MM layer as a function of frequency averaged over five random realizations. Dashed lines represent reflection and transmission of particular random realizations. (b) Absorption as a function of the damping factor γ at three different frequencies.

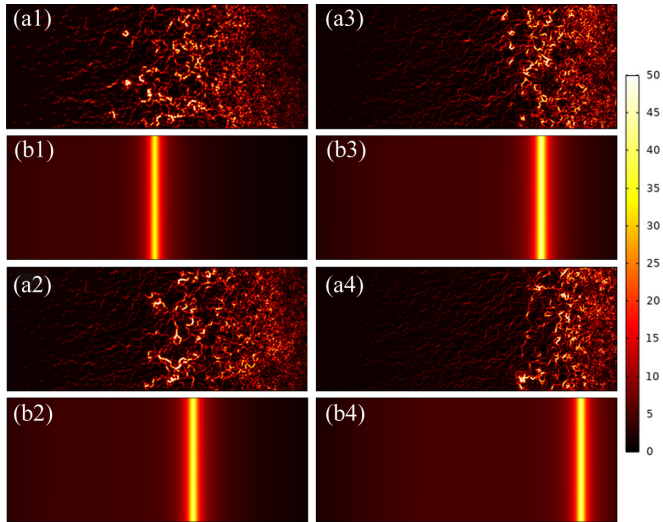


FIG. 5. Comparison between the field distributions calculated for (a1)–(a4) the random system and (b1)–(b4) the MG approximation. The frequencies were set to (a1),(b1) $\omega = 0.792\omega_p$, (a2),(b2) $\omega = 0.804\omega_p$, (a3),(b3) $\omega = 0.823\omega_p$, and (a4),(b4) $\omega = 0.842\omega_p$. The other parameters are similar to those in Fig. 3.

is in agreement with the condition given by Eq. (14) with the permittivity given by Eq. (1). Furthermore, Figs. 5 and 6 demonstrate similar trends between the resonance excitations in the random and homogenized systems. Second, although the resonant region is clearly visible, it is not very pronounced, unlike one might have expected from Fig. 2. However, it is clear that in a system constituted by discrete particles, field cannot be localized in a region smaller than the interparticle

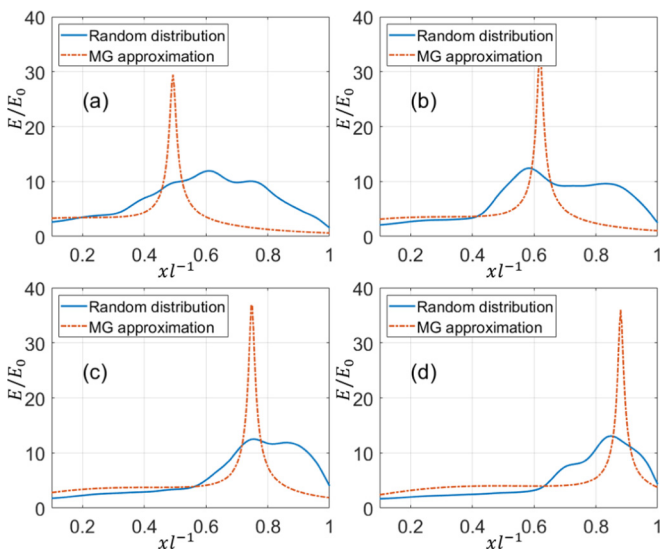


FIG. 6. Comparison between the averaged field distributions calculated for the random system (blue solid line) and the MG approximation (red dot-dashed line) for four different frequencies: (a) $\omega = 0.792\omega_p$, (b) $\omega = 0.804\omega_p$, (c) $\omega = 0.823\omega_p$, and (d) $\omega = 0.842\omega_p$. The averaging was performed over the entire y coordinate and with the Gaussian smoothing function over the x coordinate. The other parameters are similar to those in Fig. 5.

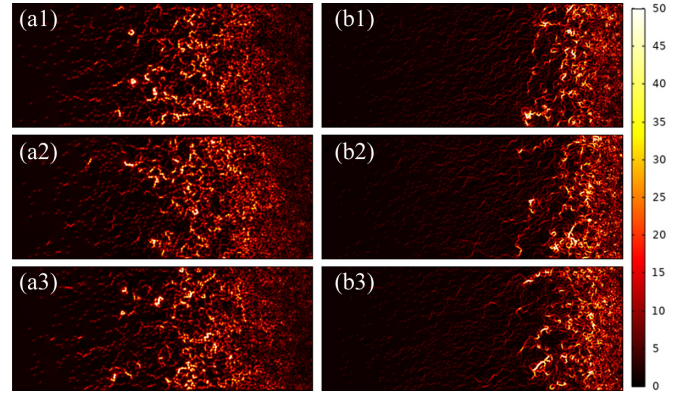


FIG. 7. Comparison between three different realizations of random distribution at two different frequencies: (a1)–(a3) $\omega = 0.785\omega_p$ and (b1)–(b3) $\omega = 0.842\omega_p$. The other parameters are similar to those in Fig. 3.

distance. Moreover, as the considered field enhancement is maintained by a collective excitation of dipoles, a significant number of dipoles is required to sustain it. The comparison presented in Fig. 5 shows that randomness plays a crucial role in the widening of the resonant region.

The widening of the resonant area is evidently attributed to the breakdown of the continuous medium approximation. Indeed, when the localization of the field reaches certain intrinsic scales of the material, the continuous medium approximation is no longer applicable. An evident intrinsic scale is the average interparticle distance. However, for the random distribution of meta-atoms, the resonant area is much wider than the average distance between the meta-atoms. It turns out that the factor that defines the size of the resonance region in this case is the fluctuations of the meta-atom concentration. Indeed, let us write the meta-atom filling fraction in the following form:

$$\rho(x, y) = \overline{\rho(x)} + \delta\rho(x, y), \quad (15)$$

where $\overline{\rho(x)}$ is the average filling fraction, which grows linearly in the x direction, and $\delta\rho(x, y)$ is the local deviation of the filling fraction from the average. Therefore, according to Eq. (3), the effective permittivity can also be expressed in a similar form,

$$\varepsilon_{\text{eff}}(x, y) = \overline{\varepsilon_{\text{eff}}(x)} + \delta\varepsilon_{\text{eff}}(x, y), \quad (16)$$

where $\overline{\varepsilon_{\text{eff}}(x)}$ is the average effective permittivity and $\delta\varepsilon_{\text{eff}}(x, y)$ is its deviation from the average. Using Eqs. (6)

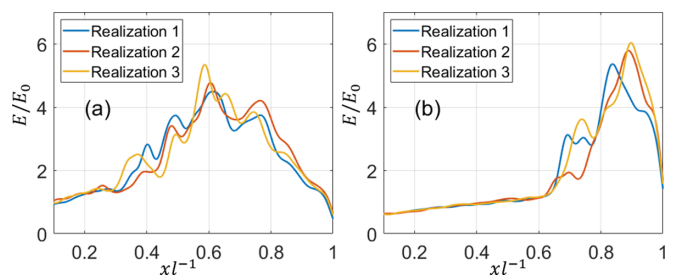


FIG. 8. Comparison between averaged field distributions calculated for the three realizations of random systems shown in Fig. 7.

and (7), the expression for the squared electric field amplitude can be written as

$$|E|^2 = |E_x|^2 + |E_y|^2 = \frac{1}{k_0^2 |\varepsilon_{\text{eff}}(x, y)|^2} \left(\left| \frac{\partial H_z}{\partial x} \right|^2 + \left| \frac{\partial H_z}{\partial y} \right|^2 \right). \quad (17)$$

As we are interested in the general properties of the random system, the expression for the electric field amplitude, given by Eq. (17), should be averaged over the random realizations of the distribution. Thus, the average amplitude will take the form

$$\langle |E|^2 \rangle = \frac{1}{k_0^2 \langle |\varepsilon_{\text{eff}}(x, y)|^2 \rangle} \left\langle \left(\left| \frac{\partial H_z}{\partial x} \right|^2 + \left| \frac{\partial H_z}{\partial y} \right|^2 \right) \right\rangle, \quad (18)$$

where the angular brackets $\langle \cdot \rangle$ represent the averaging. It is easy to see that the amplitude is maximal when the averaged permittivity is minimal. The averaged square of the effective permittivity can be rewritten as follows:

$$\langle |\varepsilon_{\text{eff}}(x, y)|^2 \rangle = (\text{Re} \overline{\varepsilon_{\text{eff}}(x)})^2 + [\text{Im} \overline{\varepsilon_{\text{eff}}(x)}]^2 + \langle [\delta \varepsilon_{\text{eff}}(x, y)]^2 \rangle. \quad (19)$$

It takes its minimal value when $[\text{Re} \overline{\varepsilon_{\text{eff}}(x_0)}]^2 = 0$, which corresponds to the condition given by Eq. (14). Thus, the maximum value of the field in the resonance region as well as its size are determined by the imaginary part of the effective permittivity and the average absolute value of the deviation of the effective permittivity from its mean. It is noteworthy that the average deviation of the permittivity, i.e., the fluctuations of the meta-atom concentration, plays a similar role to that of the imaginary part of the effective permittivity. In other words, the meta-atom density fluctuations operate as additional losses, decreasing the maximum field value in the resonance region and increasing the size of this region.

At the same time, the resonant absorption in the disordered system is still defined by Eq. (9) with $\text{Re}(\sigma) = \omega \text{Im}(\varepsilon_{\text{eff}})$. Thus, although the concentration fluctuations act like losses on the height and width of the resonance, they do not contribute to the absorption. As a result, the imaginary part of the permittivity does not cancel, and the following factor appears in the expression for the total losses:

$$W \propto \frac{\text{Im} \overline{\varepsilon_{\text{eff}}(x)}}{\sqrt{[\text{Im} \overline{\varepsilon_{\text{eff}}(x)}]^2 + \langle [\delta \varepsilon_{\text{eff}}(x, y)]^2 \rangle}}. \quad (20)$$

Therefore, fluctuations in the meta-atom concentration reduce the total resonant absorption.

To estimate the widening of the resonant area, it is possible to find the standard deviation of the permittivity. If the positions of the meta-atoms are assumed to be uncorrelated, the fluctuations in the number of meta-atoms in a given area S is $\sqrt{\bar{N}}$, where $\bar{N} = \bar{\rho} S / S_0$ is the average number of particles in this area. Thus, the filling fraction distribution can be assumed to be Gaussian with the distribution function $f(\rho) = A \exp(-\frac{(\rho - \bar{\rho})^2 S}{S_0})$. The standard deviation of the permittivity can be found as follows:

$$\langle \delta \varepsilon^2 \rangle = \int_0^\infty f(\rho) [\varepsilon_{\text{eff}}(\rho) - \overline{\varepsilon_{\text{eff}}}]^2 d\rho, \quad (21)$$

where $\varepsilon_{\text{eff}}(\rho)$ is given by Eq. (3). Applied to the considered system, Eq. (21) allows estimating the widening of the

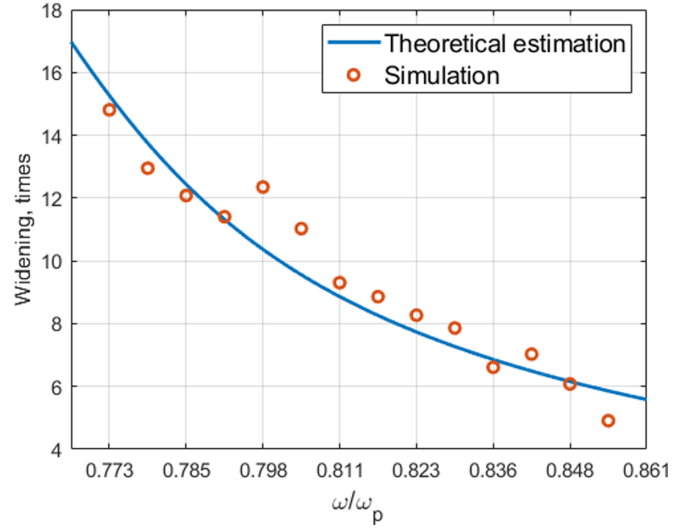


FIG. 9. Widening of the resonance region due to fluctuations in the meta-atom concentration. The theoretical estimate obtained by calculating the standard deviation of the permittivity, given by Eq. (21), is represented by the blue line; the widening obtained by direct simulation of the random system is represented by the red circles.

resonance region as $\sqrt{\text{Im} \bar{\varepsilon}^2 + \langle \delta \varepsilon^2 \rangle} / \text{Im} \bar{\varepsilon}$, which gives the ratio of the width of the resonant region in the random system to that in the homogenized system. The comparison between the widening of the resonance region calculated using Eq. (21) and that obtained using first-principles simulations is shown in Fig. 9. Despite the evaluative nature of the estimates, they are quite consistent with the numerical calculations.

As the relative fluctuations in the number of meta-atoms are proportional to the inverse square root of the number of meta-atoms itself, $\delta N / \bar{N} \propto 1 / \sqrt{\bar{N}}$, the larger the number of meta-atoms is in a given area, the smaller are the relative fluctuations. In other words, if the number of meta-atoms is increased while keeping the filling fraction constant, the role of fluctuations decreases. Finally, in the effective medium limit $N \rightarrow \infty$, the influence of the fluctuations tends to zero.

Another distinctive feature of the considered system, directly related to the concentration fluctuations, is the appearance of the hot-spot pattern outside the resonant region. Two examples of such hot spots are shown in Fig. 10.

Such a picture can be explained by the fact that due to random fluctuations in the concentration, the condition given by Eq. (14) can be satisfied at some random spots sufficiently far from the line where the real part of the average permittivity crosses zero. As a result, at these spots, resonant field excitation takes place.

From a practical point of view, systems similar to the one considered here might be advantageous as wide-range electromagnetic absorbers. Indeed, the position of the resonance region where the absorption takes place is determined by the condition given by Eq. (14), which links the frequency and the local concentration. As a result, with the change of frequency in a certain range, the resonance region changes its position in the layer of continuous variation of meta-atom concentration, thus constantly providing resonant absorption.

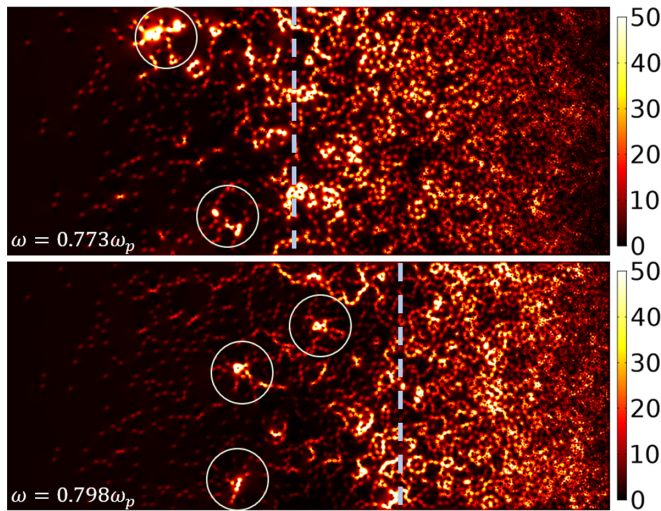


FIG. 10. Appearance of hot spots in a random distribution of meta-atoms at two different frequencies, $\omega = 0.773\omega_p$ and $\omega = 0.798\omega_p$. The hot spots are marked by white circles. The light-gray dashed line represents the line at which the condition given by Eq. (14) is satisfied. The other parameters are similar to those in Fig. 3.

According to Fig. 4(a), the considered layer provides significant suppression of both reflected and transmitted radiation in a fairly wide range of frequencies. In particular, reflection is suppressed by 10–18 dB, while transmission is suppressed by 4–11 dB. It should be noted that the thickness of the MM layer is smaller than the wavelength, ranging between 0.68 and 0.85 of the wavelength depending on the frequency. As shown in Eq. (20), the absorption can be improved by

reducing the fluctuations in the effective relative permittivity, i.e., by increasing the number of meta-atoms while simultaneously decreasing their size.

V. CONCLUSION

In this study, first-principles simulations of an inhomogeneous 2D MM with a random distribution of meta-atoms were performed. In particular, a resonant excitation of plasmalike oscillations by an oblique incidence of a linearly polarized electromagnetic wave was demonstrated. Within the effective medium approximation, such an excitation appears near the surface where the real part of the effective permittivity crosses zero. It has been shown that although the effective medium approximation becomes inadequate near the transition point, it still produces qualitatively reasonable predictions about the existence and position of the resonant mode. While the MG approximation fails to produce the width of the resonant area, analysis of the statistical properties of the system allows for accurate estimates. It has been shown that fluctuations in the meta-atom concentration in a random distribution act as additional losses. The simulations showed that the randomness of the MM causes electric field hot spots to appear outside the resonant region. The fluctuations in the meta-atom concentration can lead to an accidental satisfaction of the resonant excitation conditions of plasmalike oscillations at some point, producing hot spots.

ACKNOWLEDGMENTS

This study was supported by the French PIA project “Lorraine Université d’Excellence,” Reference No. ANR-15-IDEX-04-LUE, and the TALiSMAN project, funded by ERDF (Grant No. 2019-000214).

- [1] D. R. Smith, W. J. Padilla, D. C. Vier, S. C. Nemat-Nasser, and S. Schultz, Composite Medium with Simultaneously Negative Permeability and Permittivity, *Phys. Rev. Lett.* **84**, 4184 (2000).
- [2] R. A. Shelby, D. R. Smith, and S. Schultz, Experimental verification of a negative index of refraction, *Science* **292**, 77 (2001).
- [3] S. Linden, C. Enkrich, M. Wegener, T. Zhou, T. Kochny, and C. M. Soukoulis, Magnetic response of metamaterials at 100 terahertz, *Science* **306**, 1351 (2004).
- [4] S. Zhang, W. Fan, B. K. Minhas, A. Frauenglass, K. J. Malloy, and S. R. J. Brueck, Midinfrared Resonant Magnetic Nanostructures Exhibiting a Negative Permeability, *Phys. Rev. Lett.* **94**, 037402 (2005).
- [5] H. J. Lezec, J. A. Dionne, and H. A. Atwater, Negative refraction at visible frequencies, *Science* **316**, 430 (2007).
- [6] A. Minovich, J. Farnell, D. N. Neshev, I. McKervacher, F. Karouta, J. Tian, D. A. Powell, I. V. Shadrivov, H. H. Tan, C. Jagadish, and Y. S. Kivshar, Liquid crystal based nonlinear fishnet metamaterials, *Appl. Phys. Lett.* **100**, 121113 (2012).
- [7] A. A. Zharov, I. V. Shadrivov, and Y. S. Kivshar, Nonlinear Properties of Left-Handed Metamaterials, *Phys. Rev. Lett.* **91**, 037401 (2003).
- [8] M. Lapine, I. V. Shadrivov, D. A. Powell, and Y. S. Kivshar, Metamaterials with conformational nonlinearity, *Sci. Rep.* **1**, 138 (2011).
- [9] M. Lapine, I. V. Shadrivov, D. A. Powell, and Y. S. Kivshar, Magnetoelastic metamaterials, *Nat. Mater.* **11**, 30 (2012).
- [10] A. P. Slobozhanyuk, M. Lapine, D. A. Powell, I. V. Shadrivov, Y. S. Kivshar, R. C. McPherdan, and P. A. Belov, Flexible helices for nonlinear metamaterials, *Adv. Mater.* **25**, 3409 (2013).
- [11] W. L. Barnes, A. Dereux, and A. Ebbensen, Surface plasmon subwavelength optics, *Nature (London)* **424**, 824 (2003).
- [12] V. M. Shalaev and S. Kawata, *Nanophotonics with Surface Plasmons* (Elsevier Science, New York, 2007).
- [13] A. Zharov, Z. Viskadourakis, G. Kenanakis, V. Fierro, and A. Celzard, Control of Light Transmission in a Plasmonic Liquid Metacrystal, *Nanomaterials* **11**, 346 (2021).
- [14] M. A. Noginov, Y. A. Barnakov, G. Zhu, T. Tumkur, H. Li, and E. E. Narimanov, Bulk photonic metamaterial with hyperbolic dispersion, *Appl. Phys. Lett.* **94**, 151105 (2009).
- [15] Y. Guo, W. Newman, C. L. Cortes, and Z. Jacob, Applications of hyperbolic metamaterial substrates, *Adv. Opt. Electron.* **2012**, 452502 (2012).
- [16] A. Poddubny, I. V. Iorsh, P. A. Belov, and Y. S. Kivshar, Hyperbolic metamaterials, *Nat. Photon.* **7**, 948 (2013).
- [17] D. Schurig, J. J. Mock, B. J. Justice, S. A. Cummer, J. B. Pendry, A. F. Starr, and D. R. Smith, Metamaterial electromagnetic cloak at microwave frequencies, *Science* **314**, 977 (2006).

- [18] B. Edwards, A. Alu, M. G. Silveirinha, and N. Engheta, Experimental Verification of Plasmonic Cloaking at Microwave Frequencies with Metamaterials, *Phys. Rev. Lett.* **103**, 153901 (2009).
- [19] J. B. Pendry, Negative Refraction Makes a Perfect Lens, *Phys. Rev. Lett.* **85**, 3966 (2000).
- [20] P. A. Belov, Y. Hao, and S. Sudhakaran, Subwavelength microwave imaging using an array of parallel conducting wires as a lens, *Phys. Rev. B* **73**, 033108 (2006).
- [21] J. B. Pendry, D. Schurig, and D. R. Smith, Controlling electromagnetic fields, *Science* **312**, 1780 (2006).
- [22] U. Leonhardt, Optical conformal mapping, *Science* **312**, 1777 (2006).
- [23] Y. Tang and A. E. Cohen, Optical Chirality and Its Interaction with Matter, *Phys. Rev. Lett.* **104**, 163901 (2010).
- [24] E. Plum, V. A. Fedotov, and N. I. Zheludev, Optical activity in extrinsically chiral metamaterial, *Appl. Phys. Lett.* **93**, 191911 (2008).
- [25] W. H. Weber and G. W. Ford, Propagation of optical excitations by dipolar interactions in metal nanoparticle chains, *Phys. Rev. B* **70**, 125429 (2004).
- [26] S. Y. Park and D. Stroud, Surface-plasmon dispersion relations in chains of metallic nanoparticles: An exact quasistatic calculation, *Phys. Rev. B* **69**, 125418 (2004).
- [27] S. E. Bankov and M. D. Duplenkova, Eigenmodes of a 2D array of coupled slot lines in the impedance approximation, *J. Commun. Technol. Electron.* **62**, 827 (2017).
- [28] C. R. Simovski, P. A. Belov, A. V. Atrashchenko, and Y. S. Kivshar, Wire metamaterials: Physics and applications, *Adv. Mater.* **24**, 4229 (2012).
- [29] D. Tihon, V. Sozio, N. A. Ozdemir, M. Albani, and C. Craeye, Numerically stable eigenmode extraction in 3D periodic metamaterials, *IEEE Trans. Antennas Propag.* **64**, 3068 (2016).
- [30] M. V. Gorkunov and M. I. Ryazanov, The role of spatial dispersion near zero points of the dielectric function of cubic and uniaxial crystals, *Laser Phys.* **8**, 502 (1998).
- [31] A. Sihvola, *Electromagnetic Mixing Formulae and Applications* (Institution of Engineering & Technology, 1999), Vol. 47.
- [32] X. Liu and A. Alú, First-principle homogenization of magnetodielectric metamaterial arrays, *Proceeding of the 2011 IEEE International Symposium on Antennas and Propagation (APSURSI)* (IEEE, 2011), pp. 1522–1525.
- [33] M. G. Silveirinha, Metamaterial homogenization approach with application to the characterization of microstructured composites with negative parameters, *Phys. Rev. B* **75**, 115104 (2007).
- [34] M. Gorkunov, M. Lapine, E. Shamonina, and K. H. Ringhofer, Effective magnetic properties of a composite material with circular conductive elements, *Eur. Phys. J. B* **28**, 263 (2002).
- [35] C. Simovski, On electromagnetic characterization and homogenization of nanostructured metamaterials, *J. Opt.* **13**, 013001 (2011).
- [36] W. Zhang, Q. Song, W. Zhu, Z. Shen, P. Chong, D. P. Tsai, C. Qiu, and A. Q. Liu, Metafluidic metamaterial: A review, *Adv. Phys. X* **3**, 1 (2018).
- [37] Y. A. Urzhumov, G. Shvets, J. A. Fan, F. Capasso, D. Brandl, and P. Nordlander, Plasmonic nanoclusters: A path towards negative-index metafluids, *Opt. Express* **15**, 14129 (2007).
- [38] A. A. Zharov, A. A. Zharov, Jr., and N. A. Zharova, Liquid metacrystals, *J. Opt. Soc. Am. B* **31**, 559 (2014).
- [39] A. A. Asatryan, L. C. Botten, M. A. Byrne, V. D. Freilikher, S. A. Gredeskul, I. V. Shadrivov, R. C. McPhedran, and Y. S. Kivshar, Transmission and Anderson localization in dispersive metamaterials, *Phys. Rev. B* **85**, 045122 (2012).
- [40] M. V. Gorkunov, S. A. Gredeskul, I. V. Shadrivov, and Y. S. Kivshar, Effect of microscopic disorder on magnetic properties of metamaterials, *Phys. Rev. E* **73**, 056605 (2006).
- [41] H. Bahcivan, D. L. Hysell, and M. C. Kelley, Phase diffusion and random walk interpretation of electromagnetic scattering, *Phys. Rev. E* **68**, 021101 (2003).
- [42] R. C. McPhedran, L. C. Botten, A. A. Asatryan, N. A. Nicorovici, P. A. Robinson, and C. M. de Sterke, Calculation of electromagnetic properties of regular and random arrays of metallic and dielectric cylinders, *Phys. Rev. E* **60**, 7614 (1999).
- [43] C.-A. Guérin, P. Mallet, and A. Sentenac, Effective-medium theory for finite-size aggregates, *J. Opt. Soc. Am. A* **23**, 349 (2006).
- [44] N. Papasimakis, S. D. Jenkins, S. Savo, N. I. Zheludev, and J. Ruostekoski, Cooperative field localization and excitation eigenmodes in disordered metamaterials, *Phys. Rev. B* **99**, 014210 (2019).
- [45] E. A. Gibson, M. Pennybacker, A. I. Maimistov, I. R. Gabitov, and N. M. Litchinitser, Resonant absorption in transition metamaterials: parametric study, *J. Opt.* **13**, 024013 (2011).
- [46] E. A. Gibson, I. R. Gabitov, A. I. Maimistov, and N. M. Litchinitser, Transition metamaterials with spatially separated zeros, *Opt. Lett.* **36**, 3624 (2011).
- [47] N. G. Denisov, On a singularity of the field of an electromagnetic wave propagated in an inhomogeneous plasma, *Sov. Phys. JETP* **4**, 544 (1957).
- [48] See Supplemental Material at <http://link.aps.org/supplemental/10.1103/PhysRevA.106.013504>.doi for the visualization of the field distribution dependence on the real-time change of frequency.